Volume 4 | Number 1 | January 2017

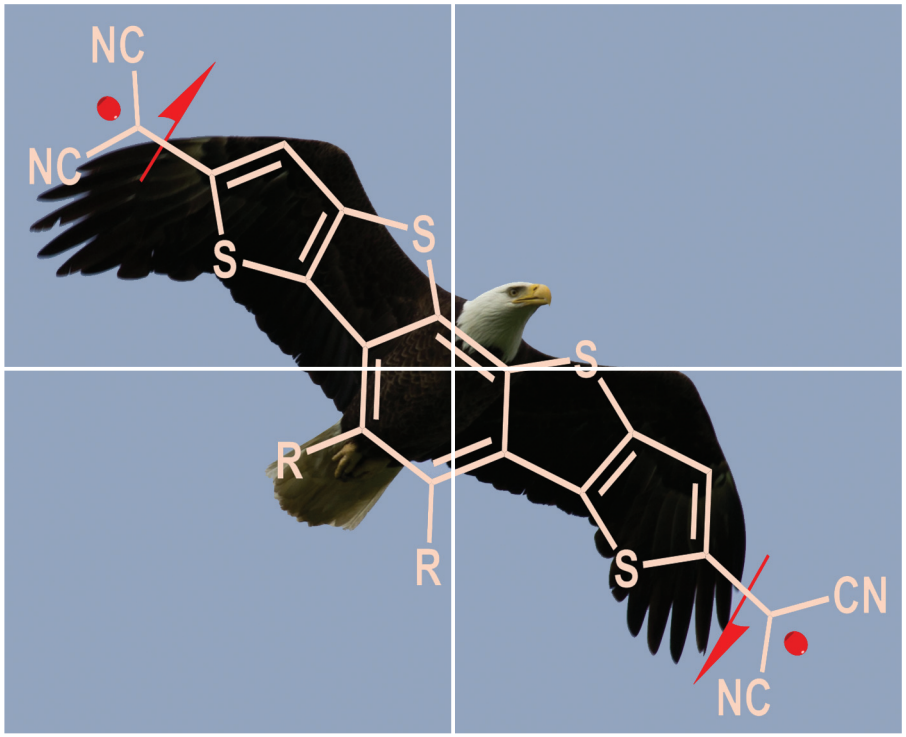

ORGANIC CHEMISTRY

FRONTIERS

Chinese Chemical Society
SIOC 1950
ROYAL SOCIETY OF CHEMISTRY

rsc.li/frontiers-organic

ORGANIC CHEMISTRY
FRONTIERS

RESEARCH ARTICLE

View Article Online
View Journal | View Issue

CrossMark click for updates

Cite this: *Org. Chem. Front.*, 2017, **4**, 18

Synthesis of a quinoidal dithieno[2,3-*d*;2′,3′-*d*]benzo[2,1-*b*;3,4-*b*′]-dithiophene based open-shell singlet biradicaloid†

Debin Xia,‡[a,b] Ashok Keerthi,‡[b,c] Cunbin An[b] and Martin Baumgarten*[b]

Received 14th September 2016,
Accepted 28th October 2016

DOI: 10.1039/c6qo00543h

rsc.li/frontiers-organic

A fused heteroacene derivative, bis(dicyanomethylene)-end-capped-dithieno[2,3-*d*;2′,3′-*d*]benzo[2,1-*b*;3,4-*b*′]-dithiophene (**4CN-DT*m*BDT**) was synthesized. Its open-shell biradical character in the ground state is studied by a combination of electron paramagnetic resonance (EPR) and nuclear magnetic resonance (NMR). Structural assignment was verified with single crystal X-ray diffraction analysis. A highly stable biradicaloid with a low energy gap and low LUMO level is achieved.

Open-shell singlet biradicaloids have been attracting tremendous interest due to their unique electronic, optical and magnetic properties for their applications in nonlinear optics, molecular spintronics, and energy storage devices.[1–5] Recently open-shell polycyclic aromatic hydrocarbons (PAHs) such as tetrabenzo[*a*,*f*,*j*,*o*]perylene,[6] cethrene,[7] zethrenes,[1,8] indenofluorene[9–12] and quinoidal rylenes[13–15] with a singlet biradical ground state have been developed. However, the open-shell structure of these molecules is vulnerable to degradation, which hampers their applications. To date, only a few molecular electronic and spintronic devices based on open-shell PAHs have been investigated.[16,17] Thus, the exploration of novel synthetic designs towards stable open-shell PAHs with tunable magnetic properties is imperative.

It is noted that the stability of the open-shell PAHs is strongly related to the additional sextet rings gained in the biradical resonance form, according to the theoretical predictions and experimental results.[1–3,18,19] Nevertheless, the synthesis of stable open-shell quinoidal oligothiophene derivatives is rarely reported.[20–22]

Recently, Ponce Ortiz and coworkers discovered that a quinoidal oligothiophene presents biradical character when the number of central thiophene rings is four or above, otherwise showing closed-shell quinoidal structures.[20] Therefore, considering the lack of synthesis protocols and challenges in thermal stability of such biradical character, we have designed a molecule **4CN-DT*m*BDT** (Scheme 1) using the planar heteroacene building block, dithieno[2,3-*d*;2′,3′-*d*]benzo[2,1-*b*;3,4-*b*′]-dithiophene (**DT*m*BDT**).[23] Three biradical resonant structures are sketched in Scheme 1. Among them, **QT1** is dominant due to the recovery of one aromatic benzene ring and two more aromatic thiophene rings. Thus **4CN-DT*m*BDT** is expected to be a stable molecule with an open-shell singlet ground state.

Herein, we report the facile synthesis of a thieno[3,2-*b*]thiophene based quinoidal **4CN-DT*m*BDT** and its biradical character is systematically investigated. As the quinoidal backbone is planar and thus having low solubility, dodecyl alkyl chains are chosen to improve the processability. Optical absorption and cyclic voltammetry (CV) measurements were applied to reveal the narrow energy gap. The variable-temperature NMR and EPR were carried out thoroughly to prove

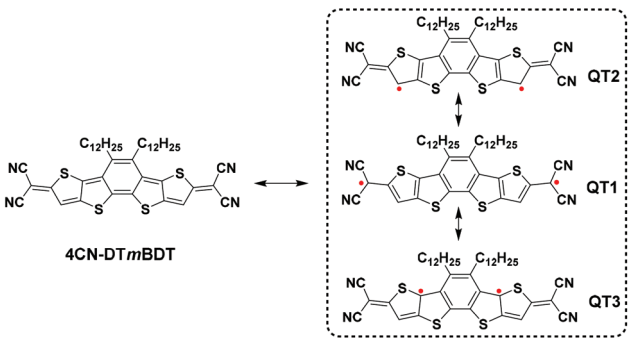

Scheme 1 Structural transformation and resonance structures of **4CN-DT*m*BDT**.

[a]*MIIT Key Laboratory of Critical Materials Technology for New Energy Conversion and Storage, School of Chemistry and Chemical Engineering, Harbin Institute of Technology, 150001 Harbin, P. R. China*
[b]*Max Planck Institute for Polymer Research, Ackermannweg 10, 55128 Mainz, Germany. E-mail: martin.baumgarten@mpip-mainz.mpg.de*
[c]*School of Physics and Astronomy Condensed Matter Physics Group, the University of Manchester, M13 9PL Manchester, UK*

†Electronic supplementary information (ESI) available: Experimental details, synthesis, characterization, single crystal data, DFT calculations and NMR spectra. CCDC 1414138. For ESI and crystallographic data in CIF or other electronic format see DOI: 10.1039/c6qo00543h

‡These authors contributed equally to this work.

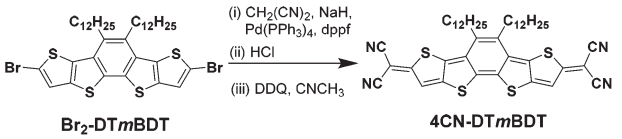

Scheme 2 Synthesis of **4CN-DT*m*BDT**.

our assumption that **4CN-DT*m*BDT** possesses an open-shell singlet ground state.

The synthesis of the tetracyano quinoidal derivative, **4CN-DT*m*BDT** was carried out through the palladium-catalyzed Takahashi coupling reaction of the precursor **Br2-DT*m*BDT**[23] with malononitrile followed by oxidation with 2,3-dichloro-5,6-dicyano-1,4-benzoquinone (DDQ) as shown in Scheme 2 with an overall yield of 68%. The dodecyl alkyl chains enable **4CN-DT*m*BDT** to have good solubility in common organic solvents such as tetrahydrofuran, dichloromethane, toluene and *N*-methylpyrrolidone. The product was characterized by ^{1}H-NMR in deuterated tetrachloroethane ($C_2D_2Cl_4$) and high-resolution MALDI-TOF MS. Thermogravimetric analysis (TGA) indicated excellent stability, with 5% weight loss occurring at 420 °C (Fig. S1†).

Single crystals of **4CN-DT*m*BDT** suitable for X-ray crystallographic analysis were obtained by slow evaporation of tetrachloroethane solution. The molecular structure was further confirmed by single crystal XRD analysis at a temperature of 193 K (Fig. 1). The backbone of the molecule is completely flat and packed in the $P\bar{1}$ (triclinic) space group. The molecules are arranged in a slipped π-stacking fashion with a π-face separation of 3.46 Å. It is found that there are significant bond length alternations in the structure. On closer inspection of such a conjugated system, only distinct double-bond character is observed rather than delocalized partial double bonds.[16] This might suggest that the ground electronic state exists mainly in the form of a closed-shell quinoidal structure at 193 K.

Intrigued by the single crystal XRD analysis, variable-temperature ^{1}H-NMR spectra of **4CN-DT*m*BDT** were recorded in $C_2D_2Cl_4$ to investigate temperature dependent differences (Fig. 2). The marked (*) resonance signal at 7.33 ppm is well-

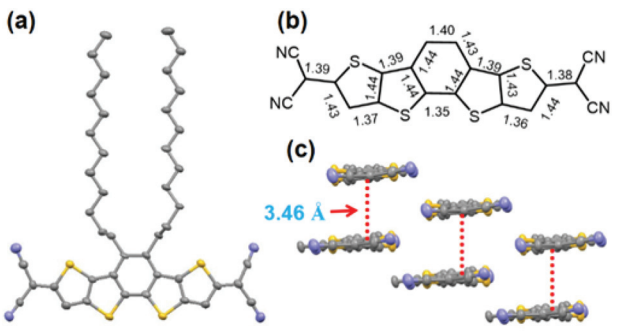

Fig. 1 Molecular structure of **4CN-DT*m*BDT**. Top view (a), (b) selected bond lengths (Å), and (c) crystal packing.

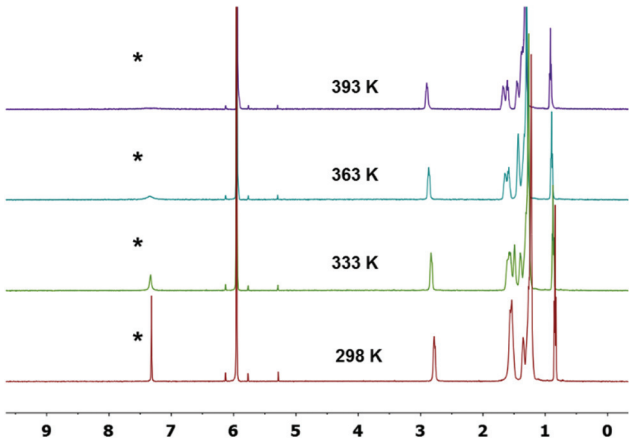

Fig. 2 Variable-temperature ^{1}H NMR spectra of **4CN-DT*m*BDT** in $C_2D_2Cl_4$.

assigned to the proton of the **DT*m*BDT** unit. This peak appeared sharply at 298 K but became broader as the temperature was increased step by step. This resonance almost disappeared at 393 K and no new peak was observed suggesting transformation to the biradical NMR inactive form. This process is entirely reversible upon cooling the sample back to 298 K, thus suggesting the high thermal stability of **4CN-DT*m*BDT**. These findings indicate a radical feature, which has also been observed in phenalenyl-, zethrene- and tetrabenzo[*a*,*f*,*j*,*o*]perylene-based biradicals, and is caused by a thermally excited triplet species.[3,6]

To further confirm the biradical nature of **4CN-DT*m*BDT**, electron paramagnetic resonance (EPR) measurement was carried out in the solid state (Fig. 3a) and in dilute solutions of toluene (Fig. S2†). As shown in Fig. 3a, **4CN-DT*m*BDT** exhibited increasing EPR signal intensities upon warming the sample from 220 to 320 K, which was in accordance with the variable-temperature ^{1}H-NMR measurements. The *g* value is 2.0028 indicating a carbon based radical. The temperature dependence of the EPR signal intensity (Fig. S2†) was analyzed using the Bleaney and Bowers equation.[24,25] The estimated singlet–triplet energy gap (ΔE_{ST}) is 2.65 kcal mol^{-1}. Consequently, both the NMR and EPR results demonstrate that compound **4CN-DT*m*BDT** has the biradical feature.

To gain insight into the electronic structure of **4CN-DT*m*BDT**, DFT calculations were performed with the geometry of single crystal structure to obtain the singlet–triplet energy gap (ΔE_{ST}) and to compare the spin density distribution. The ΔE_{ST} = −6.88 kcal mol^{-1} was calculated at the DFT unrestricted broken symmetry (BS) B3LYP/6-31g(d) level of theory[26,27] (Table S1 and Fig. S3†). As shown in Fig. 3b, C1 and C2 have the largest spin densities, as predicted in Scheme 1. Thus, the calculation results also indicate that **4CN-DT*m*BDT** exist in resonance forms between the Kekulé and biradical structures. The closed-shell DFT calculations for the quinoidal structure were also carried out to predict the frontier molecular orbital distributions and its absorption spectra through

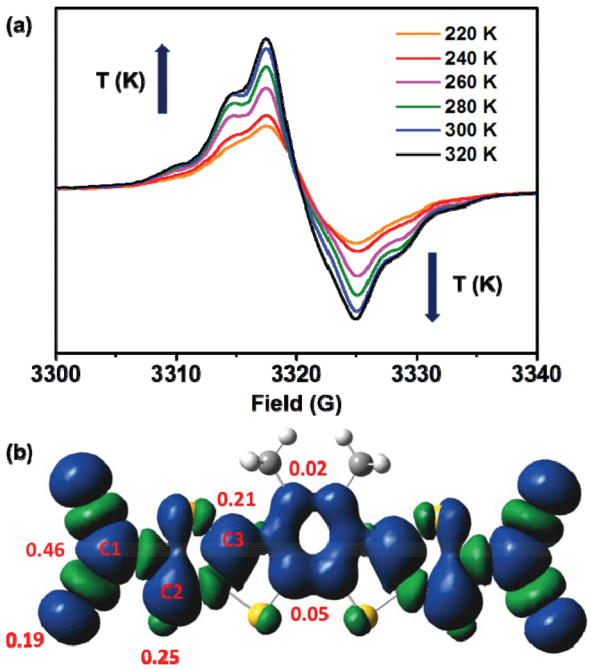

Fig. 3 (a) Variable-temperature EPR spectra of **4CN-DT*m*BDT** in the solid state. (b) Spin-density of the triplet state of **4CN-DT*m*BDT** calculated with DFT using the U3BLY/6-31G(d) level of theory.

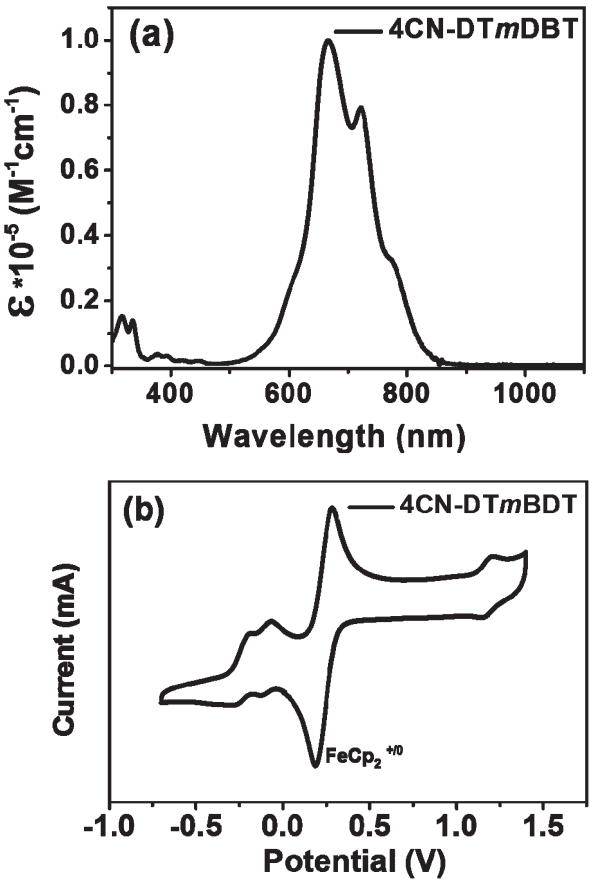

Fig. 4 (a) UV-vis absorption spectrum of **4CN-DT*m*BDT** in CH_2Cl_2 and (b) the cyclic voltammogram of **4CN-DT*m*BDT** in CH_2Cl_2 with Bu_4NPF_6 as the supporting electrolyte, at a scan rate of 100 mV s^{-1}.

B3LYP/6-31(d) and TD-SCF B3LYP/6-31G(d), respectively. The HOMO and LUMO were completely distributed all over the molecule with an energy gap of 1.34 eV (Fig. S4†). The simulated absorption spectra had two peaks at 660 nm (λ_{max}) and 318 nm with onset absorption extended over 1000 nm (Fig. S5†).

Fig. 4a illustrates the UV-vis absorption spectra of **4CN-DT*m*BDT** in dilute toluene solution. The absorption maximum appeared at 679 nm, which was red shifted around ~80 nm in comparison with the quinoidal benzo[1,2-*b*:4,5-*b*′] dithiophene derivative **DHB-QDTB** [28] (for the chemical structure, see ESI, Scheme S1†), which is due to the enlarged conjugation length. The absorption spectrum of **4CN-DT*m*BDT** had another two red-shifted shoulder peaks at 722 nm and 776 nm, respectively. The onset of absorption is related to an optical gap of 1.4 eV. The high energy peak around 320 nm was assigned to the conjugated backbone of **DT*m*BDT**. Moreover, **4CN-DT*m*BDT** showed very weak photoluminescence, further indicating the presence of biradicaloid character. Cyclic voltammetry (Fig. 4b) was employed to investigate the electrochemical properties of **4CN-DT*m*BDT**. It presented a well-resolved reversible oxidation peak at 1.12 V and two reversible reduction waves at −0.33 V and −0.47 V respectively. The ionization potential (IP) and electron affinity (EA) of **4CN-DT*m*BDT** were thus estimated to be −5.70 eV and −4.52 eV, respectively, from the onsets of the 1st oxidation and reduction peak potentials. Notably, the electrochemical energy gap (1.18 eV) of **4CN-DT*m*BDT** was similar to its analogue dicyanomethylene-substituted quinoidal dithieno[2,3-*d*;2,3-*d*] benzo[1,2-*b*;4,5-*b*′]dithiophene,[29] while the experimental values were in well agreement with the calculated HOMO and LUMO levels of the molecule (Fig. S4†).

Fascinated by the high thermal stability of **4CN-DT*m*BDT** from the TGA analysis, we have investigated possible phase transitions using differential scanning calorimetry (DSC) in the temperature range of 20 °C to 350 °C under a nitrogen atmosphere. Surprisingly, there was an exothermic phase transition at 275 °C apart from the endothermic peak at 126 °C which might be assigned to segmental melting or rearrangement. The high temperature phase transition was not reversible in the cooling cycle and did not occur in subsequent heating–cooling cycles suggesting a permanent change in the **4CN-DT*m*BDT** material. This black coloured "transformed product" from the heating cycle up to 350 °C was not soluble in any solvent even under sonication and heating conditions. MALDI-TOF analysis did not provide any clues about the "transformed product". In another experiment, heating–cooling curves for **4CN-DT*m*BDT** were recorded in the range of 20 °C to 190 °C and the endothermic phase transition (at 126 °C) was found to be reversible. Interestingly this product is quite stable which is confirmed by ^{1}H-NMR, MALDI-TOF and FT-IR analysis and in complete agreement

with **4CN-DT*m*BDT**. According to our observations (Fig. S6 and S7†) and Seki's recent work,[30] we tentatively predict that **4CN-DT*m*BDT** might go through radical polymerization at 275 °C to yield the "transformed product". The tentative polymer structure **P1** is presented in Fig. S8† by considering the following aspects: (i) in the IR spectrum (Fig. S9†), the peak representing the C≡N stretching frequency at ~2204 cm^{-1} has not changed in both **4CN-DT*m*BDT** and the polymer; (ii) the stretching frequency of aromatic C–H ($\nu_{=C-H}$ 3089 cm^{-1}) has disappeared in the polymer spectra; and (iii) the solid did not lose color thus supporting the polymerization reaction through the C2 position.[29,30]

In summary, we have successfully synthesized the conjugation elongated quinoidal molecule (**4CN-DT*m*BDT**) with 1.2 eV narrow energy gap. The exhibited open-shell biradical properties were confirmed by variable-temperature ^1H NMR and EPR analysis. The biradical **4CN-DT*m*BDT** demonstrated good thermal and electrochemical stability. Together with its planarity, efficient intermolecular π–π interaction and low singlet–triplet energy gap (ΔE_{ST}), it is expected that **4CN-DT*m*BDT** can be an ideal material for molecular electronic devices.

Acknowledgements

We acknowledge Dr Dieter Schollmeyer at Johannes Gutenberg-University for crystal structure analysis and Dr Prince Ravat at Basel University for fitting the singlet triplet energies. This work was financially supported by Transregio TR49 and the Natural Science Foundation of China (no. 51603055). We are grateful to the King Abdulaziz City of Science and Technology (KACST) for financial support.

Notes and references

1 Z. Sun, Z. Zeng and J. Wu, *Acc. Chem. Res.*, 2014, **47**, 2582–2591.
2 Z. Zeng, X. Shi, C. Chi, J. T. Lopez Navarrete, J. Casado and J. Wu, *Chem. Soc. Rev.*, 2015, **44**, 6578–6596.
3 Z. Sun and J. Wu, *J. Mater. Chem.*, 2012, **22**, 4151–4160.
4 C. Herrmann, G. C. Solomon and M. A. Ratner, *J. Am. Chem. Soc.*, 2010, **132**, 3682–3684.
5 F. Hinkel, J. Freudenberg and U. H. F. Bunz, *Angew. Chem., Int. Ed.*, 2016, **55**, 9830–9832.
6 J. Liu, P. Ravat, M. Wagner, M. Baumgarten, X. Feng and K. Müllen, *Angew. Chem., Int. Ed.*, 2015, **54**, 12442–12446.
7 P. Ravat, T. Šolomek, M. Rickhaus, D. Häussinger, M. Neuburger, M. Baumgarten and M. Juríček, *Angew. Chem., Int. Ed.*, 2016, **55**, 1183–1186.
8 Z. Sun, S. Lee, K. H. Park, X. Zhu, W. Zhang, B. Zheng, P. Hu, Z. Zeng, S. Das, Y. Li, C. Chi, R.-W. Li, K.-W. Huang, J. Ding, D. Kim and J. Wu, *J. Am. Chem. Soc.*, 2013, **135**, 18229–18236.
9 A. Shimizu, R. Kishi, M. Nakano, D. Shiomi, K. Sato, T. Takui, I. Hisaki, M. Miyata and Y. Tobe, *Angew. Chem., Int. Ed.*, 2013, **52**, 6076–6079.
10 H. Miyoshi, S. Nobusue, A. Shimizu, I. Hisaki, M. Miyata and Y. Tobe, *Chem. Sci.*, 2014, **5**, 163–168.
11 D. T. Chase, B. D. Rose, S. P. McClintock, L. N. Zakharov and M. M. Haley, *Angew. Chem., Int. Ed.*, 2011, **123**, 1159–1162.
12 D. T. Chase, A. G. Fix, S. J. Kang, B. D. Rose, C. D. Weber, Y. Zhong, L. N. Zakharov, M. C. Lonergan, C. Nuckolls and M. M. Haley, *J. Am. Chem. Soc.*, 2012, **134**, 10349–10352.
13 Z. Zeng, S. Lee, M. Son, K. Fukuda, P. M. Burrezo, X. Zhu, Q. Qi, R.-W. Li, J. T. L. Navarrete, J. Ding, J. Casado, M. Nakano, D. Kim and J. Wu, *J. Am. Chem. Soc.*, 2015, **137**, 8572–8583.
14 Z. Zeng, Y. M. Sung, N. Bao, D. Tan, R. Lee, J. L. Zafra, B. S. Lee, M. Ishida, J. Ding, J. T. López Navarrete, Y. Li, W. Zeng, D. Kim, K.-W. Huang, R. D. Webster, J. Casado and J. Wu, *J. Am. Chem. Soc.*, 2012, **134**, 14513–14525.
15 X. Zhu, H. Tsuji, K. Nakabayashi, S.-i. Ohkoshi and E. Nakamura, *J. Am. Chem. Soc.*, 2011, **133**, 16342–16345.
16 G. E. Rudebusch, J. L. Zafra, K. Jorner, K. Fukuda, J. L. Marshall, I. Arrechea-Marcos, G. L. Espejo, R. Ponce Ortiz, C. J. Gómez-García, L. N. Zakharov, M. Nakano, H. Ottosson, J. Casado and M. M. Haley, *Nat. Chem.*, 2016, **8**, 753–759.
17 H. Zhang, H. Dong, Y. Li, W. Jiang, Y. Zhen, L. Jiang, Z. Wang, W. Chen, A. Wittmann and W. Hu, *Adv. Mater.*, 2016, **28**, 7466–7471.
18 M. Randić, *Chem. Phys. Lett.*, 2014, **601**, 1–5.
19 Z. Sun, Z. Zeng and J. Wu, *Chem. – Asian J.*, 2013, **8**, 2894–2904.
20 R. Ponce Ortiz, J. Casado, S. Rodríguez González, V. Hernández, J. T. López Navarrete, P. M. Viruela, E. Ortí, K. Takimiya and T. Otsubo, *Chem. – Eur. J.*, 2010, **16**, 470–484.
21 C. Wang, Y. Zang, Y. Qin, Q. Zhang, Y. Sun, C.-a. Di, W. Xu and D. Zhu, *Chem. – Eur. J.*, 2014, **20**, 13755–13761.
22 A. Mishra, C.-Q. Ma and P. Bäuerle, *Chem. Rev.*, 2009, **109**, 1141–1276.
23 A. Keerthi, C. An, M. Li, T. Marszalek, A. G. Ricciardulli, B. Radha, F. D. Alsewailem, K. Müllen and M. Baumgarten, *Polym. Chem.*, 2016, **7**, 1545–1548.
24 B. Bleaney and K. D. Bowers, *Philos. Trans. R. Soc. London, Ser. A*, 1952, **214**, 451–465.
25 P. Ravat and M. Baumgarten, *Phys. Chem. Chem. Phys.*, 2015, **17**, 983–991.
26 K. Yamaguchi, F. Jensen, A. Dorigo and K. N. Houk, *Chem. Phys. Lett.*, 1988, **149**, 537–542.
27 M. Shoji, K. Koizumi, Y. Kitagawa, T. Kawakami, S. Yamanaka, M. Okumura and K. Yamaguchi, *Chem. Phys. Lett.*, 2006, **432**, 343–347.
28 S. Wang, M. Wang, X. Zhang, X. Yang, Q. Huang, X. Qiao, H. Zhang, Q. Wu, Y. Xiong, J. Gao and H. Li, *Chem. Commun.*, 2014, **50**, 985–987.
29 J. Li, X. Qiao, Y. Xiong, H. Li and D. Zhu, *Chem. Mater.*, 2014, **26**, 5782–5788.
30 T. Kobashi, D. Sakamaki and S. Seki, *Angew. Chem., Int. Ed.*, 2016, **55**, 8634–8638.